

## Theoretical insights into kesterite and stannite phases of $\text{Cu}_2(\text{Sn}_{1-x}\text{Ge}_x)\text{ZnSe}_4$ based alloys: A prospective photovoltaic material

S. Kumar, Durgesh Kumar Sharma, Bipin Joshi, and S. Auluck

Citation: *AIP Advances* **6**, 125303 (2016); doi: 10.1063/1.4971323

View online: <http://dx.doi.org/10.1063/1.4971323>

View Table of Contents: <http://aip.scitation.org/toc/adv/6/12>

Published by the [American Institute of Physics](#)

---

### Articles you may be interested in

[Terahertz detectors from Be-doped low-temperature grown InGaAs/InAlAs: Interplay of annealing and terahertz performance](#)

*AIP Advances* **6**, 125011125011 (2016); 10.1063/1.4971843

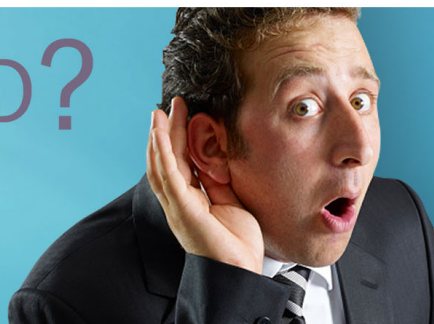
---

# HAVE YOU HEARD?

Employers hiring scientists and  
engineers trust

**PHYSICS TODAY | JOBS**

[www.physicstoday.org/jobs](http://www.physicstoday.org/jobs)



## Theoretical insights into kesterite and stannite phases of $\text{Cu}_2(\text{Sn}_{1-x}\text{Ge}_x)\text{ZnSe}_4$ based alloys: A prospective photovoltaic material

S. Kumar,<sup>1,a</sup> Durgesh Kumar Sharma,<sup>1</sup> Bipin Joshi,<sup>2</sup> and S. Auluck<sup>3</sup>

<sup>1</sup>Applied Physics Department, Faculty of Engineering and Technology,

M. J. P. Rohilkhand University, Bareilly 243 006, India

<sup>2</sup>Department of Science and Technology, New Delhi 110 016, India

<sup>3</sup>CSIR-National Physical Laboratory, Dr. K. S. Krishnan Marg, New Delhi 110 012, India

(Received 20 August 2016; accepted 15 November 2016; published online 5 December 2016)

A comparative study of kesterite (KS) and stannite (ST) phases of  $\text{Cu}_2(\text{Sn}_{1-x}\text{Ge}_x)\text{ZnSe}_4$  (CTGZSe) alloys has been carried out using a hybrid functional within the framework of density functional theory (DFT). Our calculations suggest that KS phase is energetically more stable. We find that the total energy of the KS phase decreases with increasing concentration ( $x$ ) of Ge. The calculated positive binding energies suggest that the alloy systems are stable. The formation enthalpy clearly indicates that CTGZSe alloys are thermodynamically stable and its growth can be achieved by following the route of an exothermic reaction. The calculated energy band gaps of the alloys agree well with the experimental data for the KS phase. The band offsets of KS and ST phases as a function of Ge concentration ( $x$ ) can be explained on the basis of the calculated energy band gaps. We find a slight upshift in the conduction band edges while the valence band edges remain almost the same on varying the concentration ( $x$ ) of Ge. Our results could be useful for the development of CTGZSe alloys based solar cells. © 2016 Author(s). All article content, except where otherwise noted, is licensed under a Creative Commons Attribution (CC BY) license (<http://creativecommons.org/licenses/by/4.0/>). [<http://dx.doi.org/10.1063/1.4971323>]

### I. INTRODUCTION

Environmental friendly, earth abundant and low cost elements are the parameters needed for the development of absorbing materials useful in thin film solar cells. The predicted power conversion efficiency (PCE) of ternary  $\text{Cu}(\text{In,Ga})\text{Se}_2$  (CIGSe) compound based solar cells peaks at 21.4%<sup>1</sup> and is higher than that of quaternary compound based solar cells like CGZSe and  $\text{Cu}_2\text{ZnSnSe}_4$  (CTZSe) etc. Nevertheless large scale production of CIGSe solar cells may increase the demand of In and Ga. As stocks are limited, this may increase its cost and result in a crisis. Therefore there is a necessity to look for alternate materials which can be used to develop cheap and efficient solar cells. The CGZSe and CTZSe compounds exist in two different crystal structures which are derived from zincblende (ZB) structure by making a supercell of  $1 \times 1 \times 2$  in the a, b and c directions. These are called KS (space group I4) and ST (space group I4<sub>2</sub>m) structure and differ only by the position of cations in the face centered cubic ZB structure.

Both Purdue University and IBM group researchers reported experiments predicting a PCE of  $\text{Cu}_2\text{Zn}(\text{Ge,Sn})\text{Se}_4$  alloys of 9.1% for 40% Ge doped, which is still more than the ternary compound based solar cells.<sup>2,3</sup> Recently, Mitzi *et al.*<sup>4</sup> reported PCE of 12.6% for  $\text{Cu}_2\text{ZnSnS}_x\text{Se}_{1-x}$  alloys based solar cells. This opens a window for further improvement in quaternary compound based solar cells. Wei *et al.*<sup>5</sup> studied structural and electronic properties of KS and ST phases of  $\text{Cu}_2\text{ZnSnX}_4$  (X = S and Se) using hybrid functional exchange correlation potentials. The calculated band gap of 1.5 eV

<sup>a</sup>Author to whom correspondence should be addressed. Electronic addresses: [skumar@mjpru.ac.in](mailto:skumar@mjpru.ac.in) and [drsudhirkumar.in@gmail.com](mailto:drsudhirkumar.in@gmail.com)

makes them suitable for optoelectronic devices. Repins *et al.*<sup>6</sup> calculated the electronic as well as the optical properties of CGZSe. They performed theoretical as well as experimental studies to justify their results. Moreover to the best of our knowledge neither experimental nor theoretical simulation results are available for the wurtzite-kesterite alloy phase. Furthermore, Wei *et al.*<sup>7</sup> had also shown that KS phase of pristine CTZSe and CGZSe stable than wz structure. However recently wurtzite  $\text{Cu}_2\text{Cd}_x\text{Zn}_{1-x}\text{SnS}_4$ <sup>8</sup> have been synthesized and detail investigations are carried out by Kumar *et al.*<sup>9</sup>

Wei *et al.*<sup>10</sup> investigated the structural and electronic properties of  $\text{Cu}_2\text{Zn}(\text{Sn},\text{Ge})\text{Se}_4$  and  $\text{Cu}_2\text{Zn}(\text{Sn},\text{Si})\text{Se}_4$  alloys. On the basis of calculated low formation enthalpy they concluded that Ge can be easily mixed in  $\text{Cu}_2\text{Zn}(\text{Sn},\text{Ge})\text{Se}_4$  alloys compared to Si in  $\text{Cu}_2\text{Zn}(\text{Sn},\text{Si})\text{Se}_4$  alloys, because the calculated formation enthalpy for Si doped alloys is higher than Ge doped alloys. Wada *et al.*<sup>11</sup> synthesized KS- $\text{Cu}_2\text{Zn}(\text{Sn}_{1-x}\text{Ge}_x)\text{Se}_4$  solid solution and measured lattice constants and energy band gap. We have carried out a detailed theoretical investigation for a better understanding of the stability and electronic structure description of both KS and ST phases of CTZGSe alloys. The motivation of this work is to answer some important questions. (I) Why the energy differs in both KS and ST phases although both consist of the same type and number of cations and anions ? (II) Are these structures thermodynamically favorable from crystal growth standpoint ? and (III) How these two structures can be miscible in single CTGZSe alloys ? The use of the hybrid functional potentials is essential as it can give correct energy gaps (that is gaps that agree with experiment) and total energies.

The technical aspects of *ab-initio* calculations are given in Sec. II while our calculated results along with the experimental data are presented in Sec. III. Finally, based on our results concluding remarks are summarized in Sec. IV.

## II. METHODOLOGY

The DFT calculations have been performed using the projector augmented wave (PAW)<sup>12</sup> method as implemented in the Vienna *ab-initio* Simulation Package (VASP).<sup>13,14</sup> The interaction between valence and core electrons is described within the PAW method.<sup>12</sup> Core orbitals were kept frozen to the reference states which include levels up to 3p for Cu, Zn, Ge, and Se while 4d for Sn. Brillouin zone points are sampled using a Monkhorst-Pack<sup>15</sup> mesh. The convergence criteria for the SCF cycle is  $10^{-6}$  eV (see [supplementary material](#)). For the pristine cell, we have chosen  $4 \times 4 \times 4$   $\Gamma$ -centered Monkhorst-Pack<sup>15</sup> k-point mesh while for the 64 atom supercell the mesh size is reduced to  $2 \times 2 \times 2$ . The plane wave cut off energy of 500 eV is fixed for all the calculations. We use the conjugate gradient algorithm to relax the atomic positions till the magnitude of Hellmann Feynman residual force on each atom is less than 0.01 eV/Å. It is well known that local density approximation (LDA)<sup>16</sup> and generalized gradient approximation (GGA)<sup>17</sup> underestimate energy band gaps and hence fail to give the correct description of the electronic structure near the band gap regions. To overcome this difficulty, we have used the hybrid functional exchange correlation potentials proposed by Heyd, Scuseria and Ernzerhof.<sup>18</sup> We have tuned the mixing parameter of the local and non local part of the Hartree Fock exchange. The screening parameter is equal to  $0.20 \text{ \AA}^{-1}$  while the mixing parameter ( $\alpha$ ) is tuned by the linear equation as given below:

$$\alpha = (0.0045)\beta + \gamma \quad (1)$$

where  $\gamma$  is fixed for all concentrations ( $x$ ) of Ge in CTGZSe alloys and numerically equal to 0.320 while  $\beta = 0, 1, 2, 3$  and 4 for concentration  $x = 0.00, 0.25, 0.50, 0.75$  and 1.00, (in fraction) respectively. Bekaert *et al.*<sup>19</sup> also tuned the value of  $\alpha$  by using a linear equation to explain the energy band gap variation with dopant concentration ( $x$ ) in  $\text{CuIn}_{1-x}\text{Ga}_x\text{Se}_2$  alloys. The need of Equation (1) is to obtain  $\alpha$  so that the experimental band gaps for different concentration ( $x$ ) can be reproduced. The band gap of CZTSe and CGTSe have been successfully reproduced with  $\alpha = 0.320$  and 0.338, respectively. Therefore to tune energy band gaps of intermediate concentrations ( $x$ ) we follow a linear equation (1). We used 16-atom supercell for end compounds i.e.  $x = 0.00$  and  $x = 1.00$  while calculations for doped system have been performed using a supercell of size  $2 \times 2 \times 1$  which has 64 atoms.

In calculations with defects, the prediction of the most suited site of dopant plays an important role in the ground state energy calculations. Empirically predicted sites may not give the true ground

TABLE I. Total number of configuration ( $C_{Total}$ ) and number of symmetrically inequivalent configuration (C) calculated for  $Cu_2(Sn_{1-x}Ge_x)ZnSe_4$  alloys.

Supercell size	Conc. ( $x$ )	$C_{Total}$	C
		KS/ST	KS(ST)
2x2x1	0.25	28	5(4)
2x2x1	0.50	70	9(9)
2x2x1	0.75	28	5(4)

state energy of the doped system. However, all the possible sites for dopant can be calculated by

$${}^n C_m = \frac{n!}{(n-m)! \cdot m!} \quad (2)$$

where  $n$  (total number of possible sites) and  $m$  (number of substituted dopant atoms) are real numbers. To predict energetically the most favorable site for dopant is quite a tedious and challenging job. To overcome this difficulty we use the Site Occupancy Disorder (SOD)<sup>20</sup> program which applies symmetry operations to calculate the total number of possibilities and distinguish amongst them. SOD<sup>20</sup> adapted isometric transformation for two symmetrically equivalent configurations to be one. All possible transformations can be obtained by supercell translation and space group of parent structure. The total number of configurations ( $C_{Total}$ ) for KS and ST supercell of composition  $x = 0.25$ , 0.50 and 0.75 are given in Table I. To perform DFT calculations  $C_{Total}$  is quite large but this number is drastically reduced (C) when the symmetry of lattice is taken into account as shown in Table I. The most stable configuration is predicted by total energy calculations for each symmetrically inequivalent configuration (C). The relative energy of all possible inequivalent configurations are presented in Fig. 1. The calculated configurational spectra for three configurations ( $x = 0.25$ , 0.50 and 0.75) have small energy differences, maximum of  $\sim 0.02$  eV and 0.0045 eV for KS and ST phases. The inequivalent structures for concentrations  $x = 0.25$ , 0.50 and 0.75 have small configuration energy  $\sim 10$  meV which is less than  $K_B T$  at room temperature ( $K_B$  is Boltzmann constant and T denotes temperature). Therefore it is possible that these structures may co-exist at room temperature. However, there is further need for an investigation of thermodynamical phase separation. This is beyond the scope of present paper. The SOD generated supercell for  $x = 0.50$ , shown in Fig. 2 (KS and ST phases). In ST phase the nearest neighbors distance between Ge-Sn decreases ( $5.62 \text{ \AA}$ ,  $5.59 \text{ \AA}$  &  $5.57 \text{ \AA}$ ) with increasing Ge concentration. For the KS phase, the maximum bond length for  $x = 0.50$  is  $6.88 \text{ \AA}$  while for  $x = 0.25$  &  $0.75$  it becomes  $5.65 \text{ \AA}$  and  $5.60 \text{ \AA}$ . There is a need for further investigation to explain this difference. We have earlier used SOD to obtained the most stable state for layered structure as

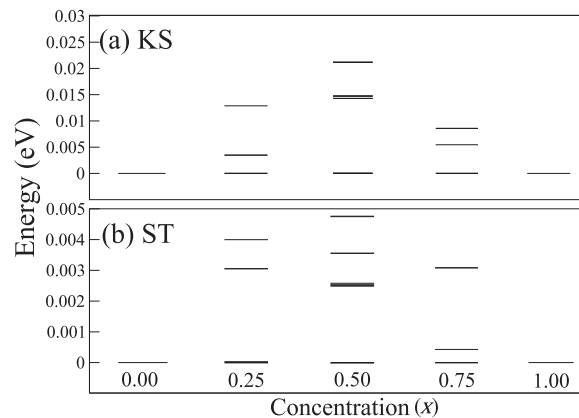


FIG. 1. The calculated configurational energies (relative to lowest energy for each composition) of inequivalent configurations generated by SOD.

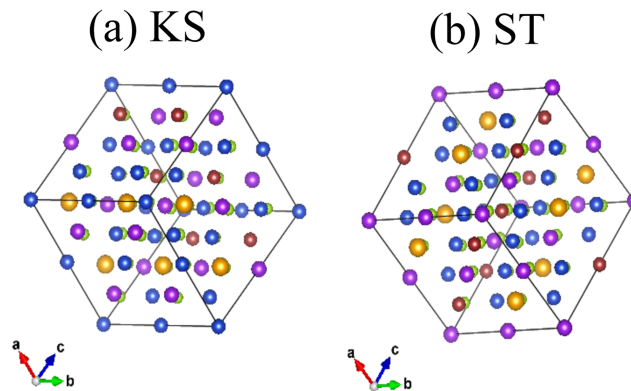


FIG. 2. SOD generated configuration of  $\text{Cu}_2(\text{Sn}_{1-x}\text{Ge}_x)\text{ZnSe}_4$  alloys for (a) KS and (b) ST phase at concentration  $x=0.50$ . Here solid sphere of color blue (Cu), brown (Ge), violet (Zn), yellow (Sn) and light green (Se), respectively.

well as wurtzite structure.<sup>9,21</sup> Further, all the calculations have been performed on the most stable predicted configuration, considered as representative for the corresponding concentration ( $x$ ).

### III. RESULTS AND DISCUSSION

#### A. Structural parameters

In our previous work,<sup>9</sup> we used several exchange correlation potentials to calculate the lattice constant. Out of these AM05 was found to be most suitable as it gave the best agreement with available experimental data. Therefore, we decided to use AM05 developed by Armiento *et al.*<sup>22,23</sup> to obtain structural parameters. Results are presented in Table II, shows  $\sim 1\%$  deviation compared to the experimental measurements.<sup>11</sup> This is very small and acceptable. The calculated lattice constants along with available experimental values<sup>11</sup> are summarized in Table II, shows decrease in the lattice constants is seen with increase of Ge concentration ( $x$ ). This can be explained, as Ge (covalent radius 1.22 Å) is smaller in size than Sn (covalent radius 1.40 Å),<sup>24</sup> hence increase of Ge dopant reduces overall the volume of the cell and thus lattice constant.

#### B. Energy difference between KS and ST phases

In the KS phase two Cu atoms are surrounded by two Sn atoms and vice versa. These two Sn atoms can repel the electronic wave function of Cu atom strongly in the crystal and this raises the overall total energy as well as energy band gap of the system. On the other hand in the ST phase the electronic wave functions of one Sn atom are repelled by only one Cu atom in the crystal (see

TABLE II. Calculated lattice constants (in Å) along with experimental data for  $\text{Cu}_2(\text{Sn}_{1-x}\text{Ge}_x)\text{ZnSe}_4$  alloys at different concentration ( $x$ ).

Conc. ( $x$ )	KS-CTGZSe		ST-CTGZSe		Experimental <sup>a</sup> (KS)	
	Present Calculations		Present Calculations		Experimental <sup>a</sup> (KS)	
	a	c	a	c	a	c
0.00(0.00)	5.699	11.308	5.698	11.311	(5.685)	(11.329)
0.25(0.20)	5.658	11.293	5.623	11.382	(5.671)	(11.290)
0.50(0.40)	5.630	11.239	5.597	11.325	(5.660)	(11.235)
0.75(0.60)	5.602	11.181	5.571	11.269	(5.648)	(11.170)
1.00(0.80)	5.590	11.079	5.569	11.099	(5.628)	(11.044)
(1.00)					(5.608)	(11.037)

<sup>a</sup>Experimental Ref. 11.

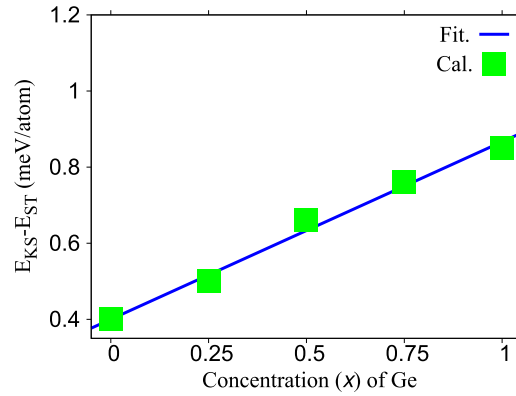


FIG. 3. Total energy difference between KS and ST with respect to Ge concentration ( $x$ ).

supplementary material for KS and ST structure files). As Cu is smaller in size than Sn, it produces less repulsion for the electronic wave function and this leads to a slightly smaller total energy and band gap. These are the reasons for the energy difference between the KS and ST phases. The calculated total ground state energies of the KS phase are 0.08%, 0.10%, 0.17%, 0.31% and 0.17% higher than that of the ST phases corresponding to concentrations (KS)( $x$ ) = 0.00, 0.25, 0.50, 0.75 and 1.00, respectively. The energy difference between these two phases is  $\sim 0.46$  meV. In Fig. 3, we have plotted the energy differences between the two phases as a function of concentration ( $x$ ). Fig. 3 indicates that with the increase of Ge concentration ( $x$ ), KS phase of CZTGSe alloys dominates. Hence, we can say that KS phase is energetically more stable than the ST phase.

### C. Binding energy

The binding energy ( $E_b$ ) of a system tells how well atoms are bound in the crystal. This plays a crucial role in explaining the stability of the system and can be calculated by using the following expression

$$E_b = E_{Cu_2(Sn_{1-x}Ge_x)ZnSe_4} - E_{Cu_2GeZnSe_4} - E_{Cu_2SnZnSe_4} \quad (3)$$

where ( $x$ ) used for dopant concentration while  $E_{Cu_2(Sn_{1-x}Ge_x)ZnSe_4}$ ,  $E_{Cu_2GeZnSe_4}$  and  $E_{Cu_2SnZnSe_4}$  are the total energies per atom at different concentrations. The calculated binding energy for concentration  $x = 0.00, 0.25, 0.50, 0.75$  and  $1.00$  of KS (ST) phases are 4.687 (4.689), 4.6406 (4.6354), 4.6093 (4.6053) and 4.5668 (4.5628) eV/atom, respectively. We do not see much difference in the calculated binding energies at different value of dopant concentration of KS and ST phases. This clearly indicates that  $E_{Cu_2(Sn_{1-x}Ge_x)ZnSe_4}$  alloys remain stable at different Ge concentrations.

### D. Formation enthalpy

The formation enthalpy  $\Delta H_f(x)$  of an alloy is a key quantity for knowing the miscibility of dopant in host compound. This can be calculated by using the following expression

$$\Delta H_f(x) = E_{Cu_2(Sn_{1-x}Ge_x)ZnSe_4}^{tot} - (1-x)E_{Cu_2GeZnSe_4}^{tot} - xE_{Cu_2SnZnSe_4}^{tot} \quad (4)$$

where  $E^{tot}$  is the total energy per atom of the pure and defected cells and ( $x$ ) represents the concentration i.e. 0.00, 0.25, 0.50, 0.75 and 1.00. The calculated  $\Delta H_f$  for different concentrations ( $x$ ) are presented in Table III. To estimate the interaction parameter, the calculated  $\Delta H_f$  presented in Fig. 4, are fitted to the following polynomial:

$$\Delta H_f(x) = \Omega x(1-x) \quad (5)$$

where  $\Omega$  is the interaction parameter which is an indicator of alloy solubility. The hexagonal symbol in Fig. 4 shows the calculated enthalpy for KS and ST structures at composition ( $x$ ) = 0.25, 0.50 & 0.75. Fitting these data with Equation (5), gives interaction parameter equal to -1.20 (-1.12) for

TABLE III. The calculated Energy band gap  $E_g^+$ , Branch Point Energy  $E_{BP}$ , Formation Enthalpy  $\Delta H_f$ , conduction  $\Delta E_c$  and valence  $\Delta E_v$  band edges for KS and ST phases of  $\text{Cu}_2(\text{Sn}_{1-x}\text{Ge}_x)\text{ZnSe}_4$  alloys (in eV). E<sup>+</sup> Present. E<sup>++</sup> Exp. Ref. 11.

Conc. (x)	KS						ST				
	$E_g^+$	$E_g^{++}$	$E_{BP}$	$\Delta E_c$	$\Delta E_v$	$\Delta H_f$	$E_g^+$	$E_{BP}$	$\Delta E_c$	$\Delta E_v$	$\Delta H_f$
0.00	0.999	0.99	3.5229	-2.5239	-3.5226	0.0000	0.836	3.4618	-2.6255	-3.4618	0.0000
0.25	1.077		3.4831	-2.4061	-3.4831	-0.0209	0.918	3.4931	-2.5511	-3.4931	-0.0220
0.50	1.206		3.4635	-2.2575	-3.4635	-0.0265	0.942	3.4362	-2.4942	-3.4362	-0.0286
0.75	1.289		3.4328	-2.1438	-3.4328	-0.0224	1.056	3.4150	-2.3588	-3.4152	-0.0250
1.00	1.357	1.35	3.3940	-2.0370	-3.3940	0.0000	1.124	3.3120	-2.1878	-3.3120	0.0000

KS (ST). The calculated  $\Delta H_f$  for KS phase is  $\sim 10$  meV lower than ST phase which suggests that KS phase is energetically more stable than ST phase. This value is quite small in comparison of  $\text{Cu}(\text{In}_x\text{Ga}_{1-x})\text{Se}_2$ <sup>25</sup> suggesting that uniform alloys of CTGZSe can be grown easily under normal temperatures. This clearly indicates that Ge dopant is well miscible in CTGZSe alloys. Hence these systems further acquire their stability with foreign dopant atoms. The calculated formation enthalpy is very small and negative, indicating that the growth of CTGZSe alloys based solar cells can be achieved by the route of exothermic reaction.

### E. Energy band gap

The calculated direct energy band gaps are presented in Table III along with the available measured data.<sup>11</sup> There is no experimental data for ST-CTGZSe alloys to compare with our results. Therefore to calculate energy band gap we use the same Equation (1) for both KS and ST phases.

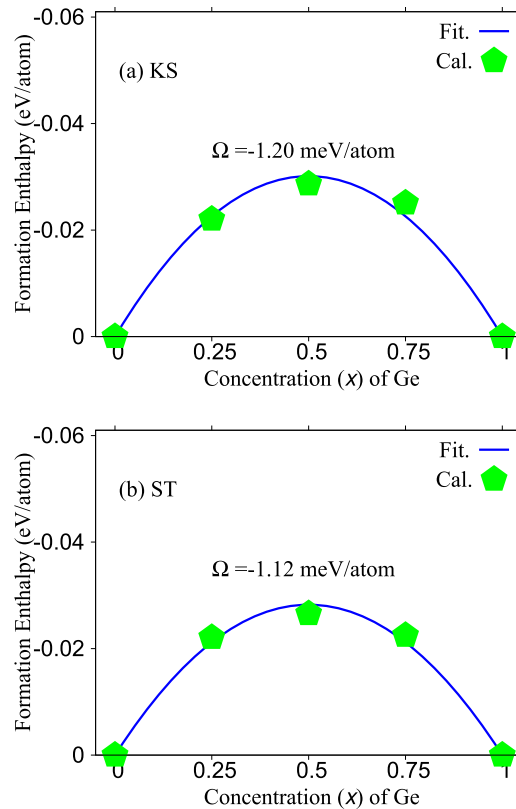


FIG. 4. The calculated formation enthalpy of  $\text{Cu}_2(\text{Sn}_{1-x}\text{Ge}_x)\text{ZnSe}_4$  alloy for (a) KS and (b) ST phases at different concentration (x).

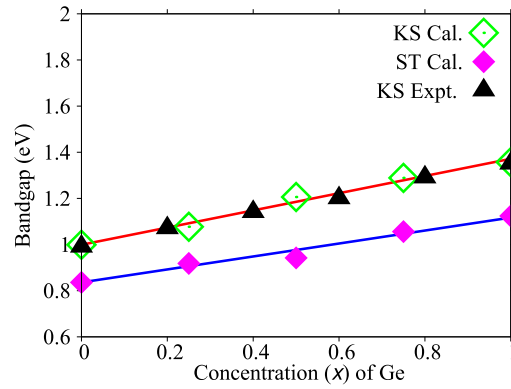


FIG. 5. The calculated energy band gap of  $\text{Cu}_2(\text{Sn}_{1-x}\text{Ge}_x)\text{ZnSe}_4$  alloys for KS and ST phases at different concentration ( $x$ ).

The calculated band gaps are plotted along with experimental data<sup>11</sup> in Fig. 5. The obtained energy band gap for KS and ST phases of CTGZSe alloys are fitted with linear equation.

$$E_g^{KS}(x) = 0.3758(x) + 0.999 \quad (6)$$

$$E_g^{ST}(x) = 0.2808(x) + 0.836 \quad (7)$$

where  $E_g$  represents the energy band gap at  $\Gamma$  point for undoped and doped cases. The slopes of KS and ST phases are 0.3758 and 0.2808 respectively. The linear variation of energy gap may be due to the small lattice mismatch between the end compounds of KS and ST phases. The linear variation of  $E_g(x)$  for KS and ST phases also suggests that the alloy is well behaved in both phases. The increase in  $E_g(x)$  with Ge concentration increases could be caused by the delocalized Sn-s orbitals in conduction band which are replaced by the more localized Ge-d orbitals. This decreases the bandwidth and the spatial confinement of the electronic wave function.

## F. Band alignment

Our calculated energy band gaps for KS phase agree very well with the experimental data. Therefore, we expect that the band offsets will also be equally good for the prediction of band alignment. We follow the approaches discussed in Refs. 26–28. The present approach has been adopted by Bechstedt *et al.*<sup>29</sup> for band offset calculation via branch point energy  $E_{BP}$ . We used the following expression to explore the electronic band edges nature of both KS and ST phases

$$E_{BP} = \frac{1}{2N_k} \sum_k \left[ \frac{1}{N_{CB}} \sum_i^{N_{CB}} \varepsilon_{c_i}(k) + \frac{1}{N_{VB}} \sum_j^{N_{VB}} \varepsilon_{v_j}(k) \right] \quad (8)$$

where  $N_k$  denotes the number of  $k$  points,  $N_{CB}$  and  $N_{VB}$  are the total number of CBs and VBs, respectively. The  $\varepsilon_{c_i}(k)$  and  $\varepsilon_{v_j}(k)$  represents the energy eigenvalues, derived from eigenwave functions.

In the present calculations, we used a single  $\Gamma$  point to evaluate  $E_{BP}$  along with three CBs i.e.  $N_{CB} = 3$  and one VB i.e.  $N_{VB} = 1$ . One has to be very careful while choosing number of bands for the calculation of band offset. Those bands which exhibit minimum dispersion have to be included to get a reliable  $E_{BP}$  otherwise results may not be accurate. The calculated  $E_{BP}$  for all concentrations average out and is used as common reference level for band edges calculations.

Figs. 6(a) and 6(b) represents the band offset for KS and ST phases, respectively. For KS phase, there is slight upshift in the CB with increase in Ge concentration ( $x$ ), because CBs are derived from the anti-bonding molecular orbitals of Sn/Ge-s and Se-4s orbitals. The p orbitals of different atoms dominate in VBs and this slightly up shifts VBs edges, as shown in Figs. 6(a) and 6(b). As the concentration ( $x$ ) of Ge increases the CB edges shifts slightly up. This is because Ge-4s orbital energy is lower than Sn-5s orbital energy. Thus overall repulsion between Sn/Ge-s and Se-4p orbitals reduces



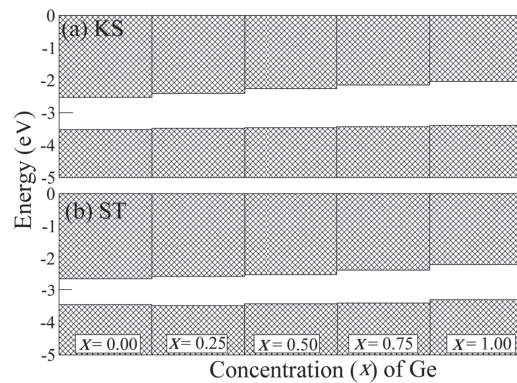


FIG. 6. The calculated band offset of alloys  $\text{Cu}_2(\text{Sn}_{1-x}\text{Ge}_x)\text{ZnSe}_4$  for (a) KS and (b) phase at different concentration ( $x$ ).

in CTGZSe alloys, resulting in a slight upshift of the CB edges. The Ge-3d orbitals lies below the Sn-4d orbitals in energy. Thus increase of Ge content produces less p-d repulsion at top of VB, resulting in a slight downshift at  $x = 0.25$  which is further elevated with increase of Ge concentration ( $x$ ). The CTGZSe based alloys may be doped via p-type dopant. However to obtain dopant characteristics, one needs to do a detailed defect formation analysis which is beyond the scope of present paper.

#### IV. CONCLUSIONS

Experimental measurements are needed for the support of theoretical predictions. Our calculated lattice constants, energy band gaps matches well with available experimental value with less than  $\sim 1\%$  deviation. The ground state energy suggests that Ge dopant is miscible quite well and also maintains its stability. The calculated binding energies for different concentrations ( $x$ ) show that overall these systems are stable. The negative formation enthalpy suggests that growth of this material can be achieved via the exothermic route. By band alignment we expect p-type doping. These results provide a benchmark to solar industry for developing more efficient solar cells based on these earth abundant elements.

#### SUPPLEMENTARY MATERIAL

See [supplementary material](#), where we have uploaded the POSCAR files for KS and ST structure along with INCAR files for force minimization and self consistent calculations. The OSZICAR file is also uploaded to confirm that accuracy has been achieved upto  $1\text{E}-06$  eV.

#### ACKNOWLEDGMENTS

This work was supported by Science and Engineering Research Board (SERB), New Delhi vide grant no. SB/S2/CMP-033/2014. SA would like to thank the High Performance Facilities (HPC) at Intra-University Accelerator Centre (IUAC) at New Delhi, Indian Institute of Mathematical Sciences (IMSC) at Chennai, CSIR-4PI at Bangaluru and Indian Institute of Technology at Kanpur.

- <sup>1</sup> P. Jackson, D. Hariskos, E. Lotter, S. Paetel, R. Wuerz, R. Menner, W. Wischmann, and M. Powalla, *Prog. Photovolt. : Res. App.* **19**, 894 (2011).
- <sup>2</sup> G. M. Ford, Q. Guo, R. Agarwal, and H. W. Hillhouse, *Chem. Mater.* **23**, 2626 (2011).
- <sup>3</sup> S. Bag, O. Gunawan, T. Gokmen, Y. Zhu, and D. B. Mitzi, *Chem. Mater.* **24**, 4588 (2012).
- <sup>4</sup> W. Wang, M. T. Winkler, O. Gunawan, T. Gokmen, T. K. Todorov, Y. Zhu, and D. B. Mitzi, *Adv. Energy Mater.* **4**, 1301465 (2014).
- <sup>5</sup> S. Chen, X. G. Gong, A. Walsh, and S.-H. Wei, *Appl. Phys. Lett.* **94**, 041903 (2009).
- <sup>6</sup> S. G. Choi, J.-S. Park, A. L. Donahue, S. T. Christensen, B. To, C. Beall, S.-H. Wei, and I. L. Repins, *Phys. Rev. Appl.* **4**, 054006 (2015).
- <sup>7</sup> S. Chen, A. Walsh, Y. Luo, J.-H. Yand, X. G. Gong, and S.-H. Wei, *Phys. Rev. B* **82**, 195203 (2010).
- <sup>8</sup> K. Ramasamy, X. Zhang, R. D. Bennett, and A. Gupta, *RSC Adv.* **3**, 1186 (2013).
- <sup>9</sup> S. Kumar, D. K. Sharma, and S. Auluck, PRB (submitted).

- <sup>10</sup> Q. Shu, J.-H. Yang, S. Chen, B. Huang, H. Xiang, X.-G. Gong, and S.-H. Wei, *Phys. Rev. B* **87**, 115208 (2013).
- <sup>11</sup> M. Morihama, F. Gao, T. Maeda, and T. Wada, *Jpn. J. Appl. Phys.* **53**, 04ER09 (2014).
- <sup>12</sup> P. E. Blöchl, *Phys. Rev. B* **50**, 17953 (1994).
- <sup>13</sup> G. Kresse and J. Furthmüller, *Phys. Rev. B* **54**, 11169 (1996).
- <sup>14</sup> G. Kresse and J. Furthmüller, *Comput. Mater. Sci.* **6**, 15 (1996).
- <sup>15</sup> H. J. Monkhorst and J. D. Pack, *Phys. Rev. B* **13**, 5188 (1976).
- <sup>16</sup> D. M. Ceperley and B. J. Alder, *Phys. Rev. Lett.* **45**, 566 (1980).
- <sup>17</sup> J. P. Perdew, K. Burke, and M. Ernzerhof, *Phys. Rev. Lett.* **77**, 3865 (1996).
- <sup>18</sup> J. Heyd, G. E. Scuseria, and M. Ernzerhof, *J. Chem. Phys.* **118**, 8207 (2003).
- <sup>19</sup> J. Bekaert, R. Saniz, B. Partoens, and D. Lamoen, *Phys. Chem. Chem. Phys.* **16**, 22299 (2014).
- <sup>20</sup> R. Grau-Crespo, S. Hamad, C. R. A. Catlow, and N. H. de Leeuw, *J. Phys. Condens. Matter* **19**, 256201 (2007).
- <sup>21</sup> S. Kumar, D. K. Sharma, and S. Auluck, *RSC Adv.* **6**, 99088 (2016).
- <sup>22</sup> A. E. Mattsson and R. Armiento, *Phys. Rev. B* **79**, 155101 (2009).
- <sup>23</sup> R. Armiento and A. E. Mattsson, *Phys. Rev. B* **72**, 085108 (2005).
- <sup>24</sup> G. L. Miessler and D. A. Tarr, *Inorganic Chemistry* (Prentice Hall, Upper Saddle River, NJ, 2003), p.45.
- <sup>25</sup> S.-H. Wei and A. Zunger, *J. Appl. Phys.* **78**, 3846 (1995).
- <sup>26</sup> F. Flores and C. Tejedor, *J. Phys. C : Solid State Phys.* **12**, 731 (1979).
- <sup>27</sup> J. Tersoff, *Phys. Rev. B* **32**, 6968 (1985).
- <sup>28</sup> M. Cardona and N. E. Christensen, *Phys. Rev. B* **35**, 6182 (1987).
- <sup>29</sup> B. Höffling, A. Schleife, F. Fuchs, C. Rödl, and F. Bechstedt, *Appl. Phys. Lett.* **97**, 032116 (2010).